JOURNAL OF MATERIALS SCIENCE **35** (2000) 3251–3256

The crystal structures of $Ba_2R_{2/3}V_2O_8$ (R = La, Nd) and $Sr_2La_{2/3}V_2O_8$; palmierite derivatives

J. M. S. SKAKLE*, A. M. COATS, J. MARR
Department of Chemistry, University of Aberdeen, Meston Walk, Aberdeen AB24 3UE, UK
E-mail: j.skakle@abdn.ac.uk

The title phases $Ba_2R_{2/3}V_2O_8$ (R = La, Nd) and $Sr_2La_{2/3}V_2O_8$, synthesised by solid state reaction of oxides at 1350°C, have structures derived from that of the palmierite-type of $Ba_3V_2O_8$; the stoichiometry is often written as $A_3RV_3O_{12}$. $Ba_2La_{2/3}V_2O_8$ is hexagonal, spacegroup $R\bar{3}m$, $\mathbf{a} = 5.75271(7)$, $\mathbf{c} = 21.0473(5)$ Å, $Z = 3$; cation ordering was determined by joint Rietveld refinement using X-ray and neutron powder diffraction data, $R_{wp} = 4.45\%$, $R_p = 6.33\%$, $\chi^2 = 6.847$. In the $Ba_3V_2O_8$ structure, Ba occupies two sites: 3a and 6c. In $Ba_2La_{2/3}V_2O_8$, Ba wholly occupies the 3a site; the 6c site contains both Ba, La and vacancies. Bond valence analysis was inconclusive, but tends to support the presence of Ba on the 3a site. $Sr_2La_{2/3}V_2O_8$ and $Ba_2Nd_{2/3}V_2O_8$ are isostructural, as confirmed by Rietveld refinement using X-ray powder diffraction data. $Ba_2R_{2/3}V_2O_8$ phases could not be synthesised for lanthanides, R, smaller than Sm.

1. Introduction

$Ba_3V_2O_8$ adopts the palmierite-type structure [1, 2] and is isostructural with a series of vanadates, arsenates, phosphates and chromates of general formula $A_3M_2O_8$ (A = Sr, Ba; M = P, As, V, Cr) [1–7] and $Pb_3V_2O_8$ [8–10]. It can be modified by substitutions at all three sites e.g. $Ba_2La_{2/3}V_2O_8$ [11], $Ba_3(W,Nb)_2O_8$ [12] and $Ba_3W_2O_6N_2$ [13]. Very recently $Ba_3Mn_2O_8$, a stable Mn^V oxide, was also reported [14].

The chemical analogue $Ba_3Nb_2O_8$ does not display the palmierite structure; instead, it is a 9R-polytype of the hexagonal perovskites [12]. The palmierite structure is, in fact, related to the 9R polytype; the oxygen atoms occupying the 9e position (1/2 0 0) in the 9R structure are replaced by oxygens in 6c (0 0 z, $z \sim 1/3$), which has the effect of creating an oxygen deficient (BaO_2) layer. Thus, whereas in the 9R polytype, structural blocks consist of units of 3 face-sharing BaO_6 octahedra linked by corner-sharing to other units, in the palmierite structure units are isolated and consist of two VO_4 tetrahedra separated by a vacant octahedron.

It is also possible to form structures intermediate between the 9R polytype and palmierite; $Ba_3MoNbO_{8.5}$ has an oxygen stoichiometry intermediate between the two structures, and indeed forms a modulated structure with ordering of octahedra and tetrahedra [15].

In addition, substitution of La for Ba in $Ba_3Nb_2O_8$ to give $Ba_3LaNb_3O_{12}$ results in a structural change to a 12R perovskite polytype, with $(hhc)_3$ packing of $(Ba/La)O_3$ layers [16].

Substitution of La for Ba in $Ba_3V_2O_8$ to give $Ba_{3-3x}La_{2x}V_2O_8$ causes no change in structure type, but produces cation vacancies. A study of the conductivity of these solid solutions under ranges of temperature and pressure revealed both ionic and electronic conductivity, the ionic conductivity being observed for a wide range of temperatures and pressures [17]. It is thus of interest to study the structure of these phases so as to provide information on the possible conduction mechanisms.

This paper reports on the structure of the cation-deficient palmierite phase $Ba_2La_{2/3}V_2O_8$ and two of its structural analogues. The phase $Ba_2La_{2/3}V_2O_8$ was originally reported as the limiting composition of a solid solution in the pseudo-binary system $Ba_3V_2O_8$-$LaVO_4$ [11] which can be written as either $Ba_{3-3x}La_{2x}V_2O_8$ ($0 \leq x \leq 2/3$) or $Ba_{4.5-3y}La_{2y}V_3O_{12}$ ($0 \leq y \leq 0.5$). $Ba_2La_{2/3}V_2O_8$ appears to be isostructural with $Ba_3V_2O_8$ and thus does not have the same structure as the chemical analogue $Ba_3LaNb_3O_{12}$ [16]. However, the $Ba_3V_2O_8$ structure has two Ba sites: 3a (0, 0, 0) and 6c (0, 0, z: $z \sim 0.2$) and the distribution of Ba and La over the two sites is not known. Due to the similarity in X-ray scattering power of Ba and La and the transparency of V to neutrons, Rietveld refinement using joint X-ray and neutron powder diffraction analysis was performed to accurately determine the structure and to elucidate the ordering of Ba, La and vacancies over the two available crystallographic sites. In addition, the isostructural compounds $Sr_2La_{2/3}V_2O_8$ and $Ba_2Nd_{2/3}V_2O_8$ were synthesised for the first time, and

* Author to whom all correspondence should be addressed.

their structures determined by Rietveld refinement using X-ray powder data.

2. Experimental

Starting materials were RE_2O_3 (RE = La, Nd, Sm, Gd) (Aldrich, 99.99%), ACO_3 (A = Ba, Sr) (Aldrich, 99.9%) and V_2O_5 (Aldrich, 99.5%); the RE_2O_3 were dried at 1000°C prior to use. Stoichiometric amounts of starting materials were ground under acetone in an agate mortar and pestle, pressed into pellets and heated at 900°C for several hours to decarbonate. The samples were reground, pressed into pellets and refired at temperatures up to 1350°C in air for 48 hours with several intermediate regrindings. The phase purity of the samples was checked by X-ray powder diffraction (XRD), initially using a Hagg-Guinier camera. In addition, quantitative electron-probe microanalysis (EPMA) was performed on a pelleted samples using a Cameca SX51 EPMA, with $BaSO_4$ for Ba L_α, LaB_6 for La L_α, V_2O_5 for V K_α. Samples were embedded in epoxy resin, polished to >1 μm and coated with carbon. A beam voltage of 20 kV and a beam current of 50 nA was used for the analysis.

Rietveld refinements using X-ray and neutron powder diffraction data were performed using GSAS Software [18]. X-ray diffraction data for Rietveld refinement were collected with a Stoe Stadi/P diffractometer in transmission mode using a small linear position sensitive detector and a germanium monochromator providing Cu $K_{\alpha 1}$ radiation ($\lambda = 1.54056$ Å, 300 K). A scan range of $10 \leq 2\theta \leq 110^\circ$ in steps of 1° was used in the refinement; the detector resolution was 0.02°, giving 4400 data points and 97 reflections. An absorption correction ($\mu \cdot t = 1.8$) was applied to the raw data. Refinement was carried out using a modified Gaussian function to model peak shape [19–21]. Initial analysis was carried out using the Stoe software packages: unit cell refinement was performed using LATREF, and theoretical powder patterns were generated using THEO. For neutron diffraction, 5 g of the compound $Ba_3LaV_3O_{12}$ were synthesised, placed in cylindrical V cans and data collected on the POLARIS diffractometer at the UK spallation neutron source, ISIS, at Rutherford Appleton Laboratory [22]. Data collected over the time-of-flight range 2000–19500 μs using the highest resolution, backscattering detectors were used in the refinement, giving 4562 data points and 2490 reflections. Peak shapes were modelled using a pseudo-Voigt function and an asymmetry parameter was refined.

3. Results and discussion

Samples were prepared according to the solid solution formula $Ba_{4.5-3y}La_{2y}V_3O_{12}$ with $y = 0$, 0.1, 0.2, 0.25, 0.3, 0.4, 0.5, 0.55, 0.6, 0.7. Unit cells were indexed on the basis of the $Ba_3V_2O_8$ unit cell [23]; the variation of unit cell parameters with composition is shown in Fig. 1. The variation is linear up to $y = 0.5$, and in good agreement with the results of Antonov *et al.* [11]. Although no impurities could be detected in the X-ray powder pattern for $y = 0.55$, the unit cell parameters were close to those of $y = 0.5$, which suggests that the limit of the solid solution is close to $y = 0.5$. For higher values of y, $LaVO_4$ was clearly present in the diffraction patterns together with the solid solution end-member.

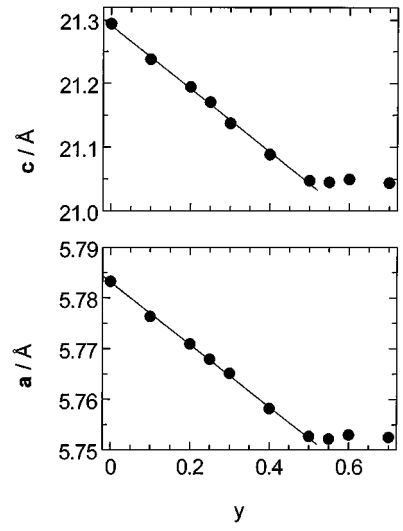

Figure 1 Variation of unit cell parameters with y in $Ba_{4.5-3y}La_{2y}V_3O_{12}$. $y = 0 = Ba_3V_2O_8$, $y = 0.5 = Ba_2La_{2/3}V_2O_8$.

TABLE IA Indexed powder pattern for $Sr_2La_{2/3}V_2O_8$: **a** = 5.6295 (2) Å, **c** = 19.9534 (12) Å

2θ(obs)	h	k	l	Int.	d (obs)	d (calc)
18.729	1	0	1	4.7	4.7339	4.7359
28.882	0	1	5	100.0	3.0887	3.0880
31.771	1	1	0	90.6	2.8142	2.8147
37.119	0	2	1	1.5	2.4201	2.4196
37.962	2	0	2	6.4	2.3682	2.3680
40.588	0	1	8	3.2	2.2209	2.2205
40.668	0	0	9	1.1	2.2167	2.2170
41.191	0	2	4	6.4	2.1897	2.1901
42.011	1	1	6	7.4	2.1489	2.1485
43.462	2	0	5	28.3	2.0804	2.0802
49.298	1	0	10	21.8	1.8469	1.8467
49.662	2	1	1	1.7	1.8342	1.8349
54.839	1	2	5	18.4	1.6727	1.6729
56.582	3	0	0	9.4	1.6252	1.6251
59.848	0	2	10	5.6	1.5441	1.5440
63.676	0	3	6	1.3	1.4602	1.4601
66.361	2	2	0	6.5	1.4075	1.4074
69.358	2	1	10	8.2	1.3538	1.3537
73.960	3	1	5	4.5	1.2805	1.2806
79.648	1	1	15	3.3	1.2028	1.2027
82.719	0	4	5	1.3	1.1657	1.1657
86.982	1	3	10	2.3	1.1192	1.1193
91.318	2	3	5	1.5	1.0770	1.0770
92.773	4	1	0	1.5	1.0639	1.0639
96.901	0	3	15	1.2	1.0293	1.0293

Other chemical analogues were also prepared; unit cells for $Sr_2La_{2/3}V_2O_8$ and $Ba_2Nd_{2/3}V_2O_8$ were refined and fully indexed powder patterns are given in Table IA and B. For R = Sm, Gd, $A_2R_{2/3}V_2O_8$ could not be synthesised; instead, mixtures of $Ba_3V_2O_8$ and RVO_4 were produced. There was no evidence of any solid solubility from the X-ray films, although it is possible that very small amounts of Sm/Gd could substitute for Ba.

Quantitative EPMA analysis was performed on a pelleted sample of $Ba_3LaV_3O_{12}$ ($y = 0.5$) [equivalent to $Ba_2La_{2/3}V_2O_8$]; oxygen content was not determined directly but was calculated by stoichiometry for

TABLE IB Indexed powder pattern for $Ba_2Nd_{2/3}V_2O_8$: **a** = 5.6336 (2) Å, **c** = 20.0875 (8) Å

2θ (obs)	h	k	l	Int.	d (obs)	d (calc)
18.697	1	0	1	11.5	4.7420	4.7410
25.438	1	0	4	11.5	3.4986	3.4993
28.754	0	1	5	100.0	3.1022	3.1014
31.734	1	1	0	90.2	2.8174	2.8168
37.100	0	2	1	3.3	2.4213	2.4217
37.931	2	0	2	3.6	2.3701	2.3705
40.368	0	1	8	7.3	2.2325	2.2326
	0	0	9			2.2319
41.110	0	2	4	10.1	2.1939	2.1943
41.871	1	1	6	4.9	2.1557	2.1554
43.354	2	0	5	35.4	2.0854	2.0851
48.991	0	2	7	19.7	1.8578	1.8586
	1	0	10			1.8575
49.598	2	1	1	2.6	1.8365	1.8363
52.245	2	0	8	8.1	1.7495	1.7497
	1	1	9			1.7494
52.852	2	1	4	3.1	1.7308	1.7310
54.731	1	2	5	22.9	1.6757	1.6759
56.552	3	0	0	11.8	1.6260	1.6263
59.558	2	1	7	7.6	1.5509	1.5513
	0	2	10			1.5507
66.309	2	2	0	8.1	1.4085	1.4084
68.041	0	1	14	1.9	1.3768	1.3765
69.078	2	1	10	9.6	1.3586	1.3584
70.224	0	0	15	1.1	1.3392	1.3392
71.757	0	3	9	2.4	1.3143	1.3144
72.259	1	3	4	1.2	1.3064	1.3066
73.829	3	1	5	6.9	1.2825	1.2824
77.048	2	0	14	1.2	1.2367	1.2368
79.118	1	1	15	5.1	1.2095	1.2094
80.582	3	1	8	2.1	1.1911	1.1912
	2	2	9			1.1911
82.589	0	4	5	2.4	1.1672	1.1671
85.728	1	2	14	1.5	1.1323	1.1324
86.678	4	0	7	3.5	1.1223	1.1225
	1	3	10			1.1223
91.182	2	3	5	2.9	1.0783	1.0782
92.682	4	1	0	2.9	1.0647	1.0647
95.258	3	2	7	1.1	1.0426	1.0428
	4	0	10			1.0426
96.350	0	3	15	2.7	1.0337	1.0338

each point analysed, assuming fixed valence for each cation; 3+ for La, 2+ for Ba and 5+ for V. The results revealed a single phase sample of stoichiometry $Ba_{3.03(2)}La_{1.00(1)}V_{3.00(1)}O_{12.02(1)}$, thus confirming the nominal composition. A sample with $y = 0.55$ was also analysed; the sample was multi-phase with a main phase of stoichiometry $Ba_{2.99(2)}La_{1.00(1)}V_{3.01(1)}O_{12.01(1)}$, confirming the solid solution limit as $y = 0.5$.

The structure of $Ba_2La_{2/3}V_2O_8$ was analysed using joint Rietveld refinement using X-ray and neutron powder diffraction data, with starting parameters from the structure of $Ba_3V_2O_8$ [24] (Table II), in which Ba occupies the 3a and 6c positions. In the starting model for $Ba_2La_{2/3}V_2O_8$, Ba and La were distributed equally over the two sites in the ratio 0.6667 : 0.2222. The refinement of occupancies was constrained by the expected stoichiometry; all other parameters were allowed to refine freely. The refinement converged successfully to give final site occupancies of: Ba1 0.98(8), La1 0.03(7); Ba2 0.51(7), La2 0.32(7). It was thus concluded that the 3a site was fully occupied by Ba, and that the 6c site was occupied by 1/2 Ba and 1/3 La. These values were held fixed in the final refinement, which converged to give

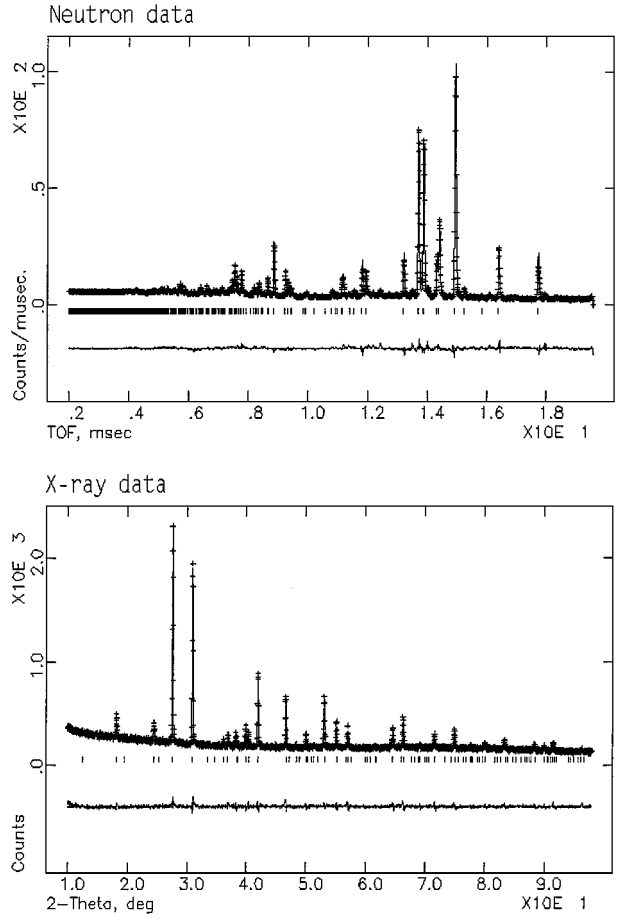

Figure 2 Observed (crosses), calculated (solid line) and difference profiles after Rietveld refinement of $Ba_2La_{2/3}V_2O_8$ using neutron and X-ray powder diffraction data.

TABLE II Atomic parameters for $Ba_3V_2O_8$, from [24], used as starting model for refinements

		x/a	y/b	z/c
Ba1	3a	0	0	0
Ba2	6c	0	0	0.2053
V1	6c	0	0	0.4076
O1	6c	0	0	0.3280
O2	18h	0.1622	$-x$	0.5642

$R_{wp} = 4.45\%$. The final observed, calculated and difference profiles are shown in Fig. 2, the crystallographic data for $Ba_2La_{2/3}V_2O_8$ obtained by Rietveld refinement given in Table IIIA and a selection of bond lengths and angles in Table IIIB.

The structure of $Ba_2La_{2/3}V_2O_8$ was used as a starting model for the refinement of the structures of $Sr_2La_{2/3}V_2O_8$ and $Ba_2Nd_{2/3}V_2O_8$ using X-ray powder diffraction data. Again, these converged successfully; the refined data and bond lengths are given in Tables IVA and B and VA and B, respectively. Both compounds are thus isostructural with the palmierite structure of $Ba_3V_2O_8$ and with $Ba_2La_{2/3}V_2O_8$.

The structure of $Ba_2La_{2/3}V_2O_8$ and its analogues is shown in Fig. 3. Each cation site in the structure has a different co-ordination environment: Ba1 is octahedral, V is tetrahedral and Ba/La is coordinated to 10 oxygen atoms with one short bond to O1, 6 long bonds to O2 and 3 medium bonds to O2. This unusual coordination environment is shown in Fig. 4a. The Ba/La polyhedron

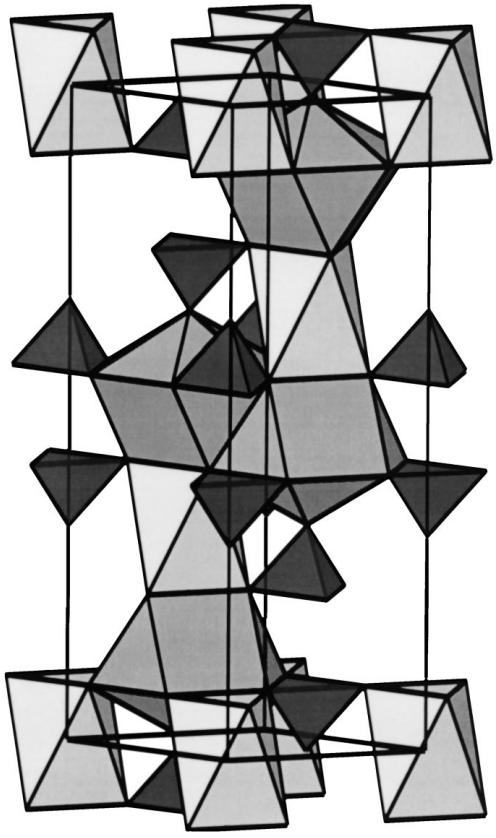

Figure 3 Structure of $Ba_2La_{2/3}V_2O_8$ and analogues. Dark triangles are VO_4 tetrahedra, mid-grey polyhedra are BaO_6 octahedra and light-grey polyhedra are $(Ba,La)O_{10}$.

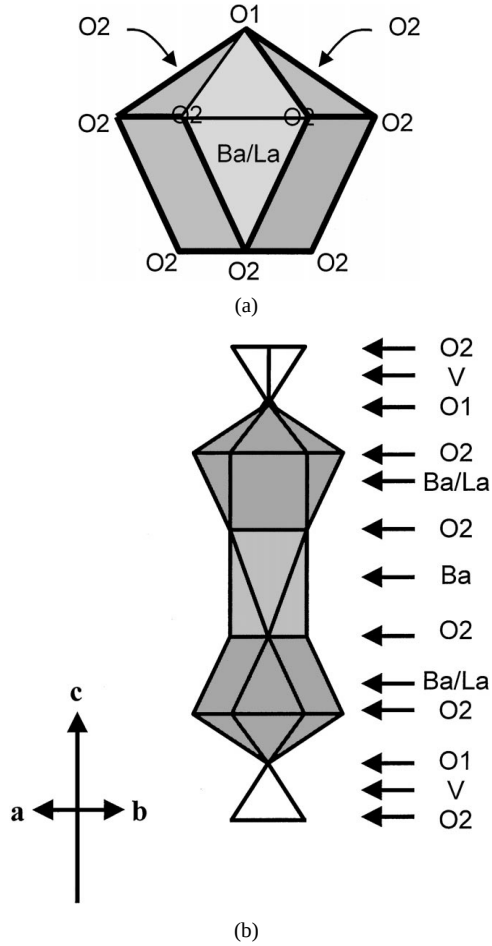

Figure 4 (a) Co-ordination environment of 6c site of Ba/La; (b) Diagram showing polyhedral linkage in $A_2R_{2/3}V_2O_8$. White triangles are VO_4, dark grey polyhedra are $(A,R)O_{10}$ and light grey polyhedra are AO_6.

TABLE IIIA Results of joint X-ray and neutron refinement for $Ba_2La_{2/3}V_2O_8$

	Occ ([a])	*x*/*a*	*y*/*b*	*z*/*c*	U_{iso} (Å^3)
Ba1	1	0	0	0	.0253 (9)
Ba2	0.5	0	0	0.20442 (13)	.0225 (6)
La2	0.3333	0	0		
V1	1	0	0	0.4109 (8)	.006 (3)
O1	1	0	0	0.3271 (2)	.0243 (12)
O2	1	0.1624 (2)	$-x$	0.57027 (8)	.0268 (4)

$R_{wp} = 4.45\%$; $R_p = 6.33\%$; $\chi^2 = 6.847$.
Spacegroup R3m, $Z = 3$. **a** = 5.75271 (7) Å, **c** = 21.0473 (5) Å, V = 603.215 (14) Å^3.
[a]Sites were originally refined to the following values (constrained by stoichiometry) but held fixed at the "ideal values" above in the final refinement: Ba1 0.98 (7), La1 0.03 (7): Ba2 0.51 (7), La2 0.32 (7).

TABLE IIIB Selected bond lengths and angles for $Ba_2La_{2/3}V_2O_8$

		Bond length				Bond angles
V	O1	1.764 (17)	O1-	V-	O2	103.8 (5)
	O2 × 3	1.666 (4)	O2-	V-	O2	114.5 (6)
Ba1	O2 × 6	2.6490 (15)				
Ba/La2	O1	2.582 (5)				
	O2 × 6	2.9570 (13)				
	O2 × 3	2.841 (3)				

TABLE IVA Rietveld refinement results for $Sr_2La_{2/3}V_2O_8$

	Occ	*x*/*a*	*y*/*b*	*z*/*c*	U_{iso} (Å^3)
Sr1	1	0	0	0	.0470 (12)
Sr2	0.5	0	0	.19821 (12)	.0457 (9)
La2	0.3333	0	0		
V1	1	0	0	.4027 (2)	.0678 (13)
O1	1	0	0	.3100 (7)	.086 (4)
O2	1	.1620 (5)	$-x$	.5767 (4)	.083 (2)

$R_{wp} = 6.24\%$; $R_p = 7.22\%$; $\chi^2 = 17.306$.
Spacegroup R3m, $Z = 3$. **a** = 5.6295 (2) Å, **c** = 19.9534 (12) Å.

TABLE IVB Selected bond lengths and angles for $Sr_2La_{2/3}V_2O_8$

		Bond length				Bond angles
V	O1	1.850 (14)	O1-	V1-	O2	104.6 (3)
	O2 × 3	1.632 (4)	O2-	V1-	O2	113.9 (3)
Sr1	O2 × 6	2.452 (6)				
Sr/La2	O1	2.230 (14)				
	O2 × 6	2.956 (4)				
	O2 × 3	2.730 (7)				

edge-shares with 3 BaO_6 octahedra and corner shares with 3 VO_4 tetrahedra around its equatorial plane, and corner-shares with 1 VO_4 at its apex and via the three, lower O2 atoms (Fig. 4a). The BaO_6 octahedra link the Ba/LaO_{10} polyhedra by face sharing, thus building up VO_4-Ba/La_{10}-BaO_6-Ba/LaO_{10}-VO_4 units along the *c*-axis with a central 3-fold axis (Fig. 4b). Each VO_4 tetrahedra corner-shares with 3 BaO_6 and 1 Ba/LaO_{10}.

Comparison with the $Ba_3V_2O_8$ structure [2] reveals that the VO_4 are more distorted in $Ba_2La_{2/3}V_2O_8$, with bond lengths of ~1.76 and 1.67 Å together with angles

TABLE VA Rietveld refinement results for $Ba_2Nd_{2/3}V_2O_8$

	Occ	*x*/*a*	*y*/*b*	*z*/*c*	U_{iso} (Å^3)
Ba1	1	0	0	0	.0443 (16)
Ba2	0.5	0	0	.20516 (15)	.0433 (15)
Nd2	0.3333	0	0		
V1	1	0	0	.4077 (4)	.065 (2)
O1	1	0	0	.3276 (8)	.084 (7)
O2	1	.1610 (8)	$-x$	.5649 (8)	.087 (4)

$R_{wp} = 6.50\%$; $R_p = 7.44\%$; $\chi^2 = 13.040$.
Spacegroup R3m, $Z = 3$. **a** = 5.6336 (2) Å, **c** = 20.0875 (8) Å.

TABLE VB Selected bond lengths and angles for $Ba_2Nd_{2/3}V_2O_8$

		Bond length				Bond angles
V	O1	1.609 (18)	O1-	V1-	O2	109.3 (5)
	O2 × 3	1.665 (7)	O2-	V1-	O2	109.6 (6)
Ba1	O2 × 6	2.647 (13)				
Ba/Nd2	O1	2.460 (16)				
	O2 × 4	2.867 (5)				
	O2 × 3	2.672 (13)				

103.8° and 114.5° compared with the more equal distribution of 1.70 and 1.71 Å, angles 108.8 and 109.2°, in $Ba_3V_2O_8$. The Ba1-O2 bond length is short, at 2.65 Å, compared with the expected value of 2.75 Å[25], but is far longer than an expected La-O bond length (2.432 Å). This might lead to the conclusion that some La occupies the Ba1 site, especially since the Ba/La2-O bond lengths are very close to those reported for $Ba_3V_2O_8$, in which only Ba occupies the site. However, the results of the refinement of site occupancies clearly indicate the presence of La only on the 6c site. Refinements based on models with La occupying the 3A site converged, but with significantly higher *R*-values (>5%).

Bond valences for the $Ba_2La_{2/3}V_2O_8$ structure were calculated from the bond lengths using appropriate constants from Brown [26] and are given in Table VIA. The values are close to the expected valence at each site, but are not wholly conclusive. This may be because the valence sum rule is not strictly obeyed by "constrained" structures such as perovskites, i.e. those in which many atoms lie on special positions [27] as is the case in this structure.

TABLE VIA Bond valence sums for cations in $Ba_2La_{2/3}V_2O_8$

		Bond length	Bond valence	Cation valence	Valence sum
V	O1	1.764 (17)	1.0805	5	5.42
	O2 × 3	1.666 (4)	1.4463		
Ba1	O2 × 6	2.6490 (15)	0.3686	2	2.21
Ba/La2	O1	2.582 (5)	0.3272		
	O2 × 6	2.9570 (13)	0.1296	2	1.62
	O2 × 3	2.841 (3)	0.1703	(Average)	

To examine this further, bond valence sums (BVS) for various models of Ba/La distribution were calculated. These are reported in Table VIB, with summed differences between the expected and calculated valence sums given in the final column for each model. It can be seen that those which have predominantly La on the 3a sites have the poorest BVS, whereas those with predominantly Ba on 3a are significantly better, although the deduced model gives a poorer fit that the two other models. However, this does support the conclusion that Ba does occupy the 3a site. It is also notable from this analysis that only two models give an even valence distribution over the two sites, Models 1 & 5 (Table VI), as in the parent structure $Ba_3V_2O_8$. Comparing these two models, Model 5, which is the one deduced from Rietveld refinement, has the better BVS fit.

Acknowledgements

We thank EPSRC for microprobe funding and also, with ISIS, for access to neutron facilities at Rutherford Appleton Laboratory.

References

1. A. DURIF, *Acta Cryst.* **12** (1959) 420.
2. P SÜSSE and M. J. BUERGER, *Z. Krist.* **131** (1970) 161.
3. H. MATTAUSCH and H. MULLER-BUSCHBAUM, *Z. Naturforsch.* **B27** (1972) 739.
4. C. H. PARK and K. BLUHM, *ibid.* **B51** (1996) 722.
5. W. CARRILLO-CABRERA and H. G. VON SCHNERING, *Z. Krist.* **205** (1993) 271.
6. W. H. ZACHARIASEN, *Acta Cryst.* **1** (1948) 263.
7. J. M. LONGO and L. R. CLAVENNA, *Ann. NY Acad. Sci.* **272** (1976) 45.
8. H. BACHMANN, *Naturwiss.* **39** (1952) 570.
9. *Idem., Neues Jahr. Miner. Monatsch.* **1953** (1953) 209.
10. J. M. KIAT, P. GARNIER and M. PINOT, *J. Sol. State Chem.* **91** (1991) 339.
11. V. A. ANTONOV, P. A. ARSEN'EV and KH. G. TADZHI-AGLAEV, *J. Inorg. Chem.* **31** (1986) 1409.
12. S. KEMMLER-SACK and U. TREIBER, *Z. Anorg. Allg. Chem.* **478** (1981) 198.
13. P. SUBRAMANYA HERLE, M. S. HEGDE and G. N. SUBBANNA, *J. Mater. Chem.* **7** (1997) 2121.
14. M. T. WELLER and S. J. SKINNER, *Acta Cryst.* **C55** (1999) 154.
15. E. GARCIA-GONZALEZ, M. PARRAS and J. M. GONZALEZ-CALBET, *Chem. Mater.* **10** (1998) 1576.

TABLE VIB Bond valence sums for various cation distributions in $Ba_2La_{2/3}V_2O_8$

Model	Cation distribution Site 1	Cation distribution Site 2	BVS Site 1	BVS Site 2	Average valence Site 1	Average valence Site 2	Difference[a]
1	2/3 La	1 Ba	1.0842	2.1429	2	2	1.06
2	2/3 La : 1/3 Ba	5/6 Ba	1.8214	1.7857	2.6667	1.6667	0.96
3	2/3 Ba	2/3 Ba : 1/3 La	1.4744	1.9725	1.3333	2.3333	0.50
4	2/3 Ba : 1/3 La	2/3 Ba : 1/6 La	2.0164	1.7006	2.3333	1.8333	0.45
5	1 Ba	1/2 Ba : 1/3 La	2.2116	1.6154	2	2	0.60

[a] ***Difference*** $= |(Average\ Valence - BVS)_{Site1}| + |(Average\ Valence - BVS)_{Site2}|$

16. H. J. ROTHER, S. KEMMLER-SACK, U. TREIBER and W. R. CYRIS, *Z. Anorg. Allg. Chem.* **466** (1980) 131.
17. I. A. LEONIDOV, O. N. LEONIDOVA and A. A. FOTIEV, *Sov. Electrochem.* **28** (1992) 1241.
18. R. B. VON DREELE and A. C. LARSON, GSAS-Generalised crystal structure analysis system, Neutron Scattering Centre, Los Alamos National Laboratory, California, 1998.
19. C. J. HOWARD, *J. Appl. Cryst.* **15** (1982) 615.
20. M. J. COOPER and J. P. SAYER, *J. Appl. Cryst.* **8** (1975) 615.
21. J. THOMAS, *Appl. Cryst.* **10** (1977) 12.
22. R. I. SMITH and S. HULL, Report RAL-94-115, Rutherford Appleton Laboratory, Oxon, UK, 1994.
23. PDF card no. 29-211, International Centre for Diffraction Data, Newtown Square, Pennsylvania, USA.
24. G. LIU and J. E. GREEDAN, *J. Sol. State Chem.* **110** (1994) 274.
25. R. D. SHANNON, *Acta Cryst.* **A32** (1976) 751.
26. I. D. BROWN, in "Structure and Bonding in Crystals Vol. II," edsited by M. O'Keeffe and A. Navrotsky (Academic Press, 1981).
27. *Idem., J. Sol. State Chem.* **90** (1991) 155.

Received 15 July
and accepted 10 December 1999